DOI 10.24425/aee.2024.150898

An experiment method of maximum power point tracking for photovoltaic panel based on hardware in loop simulation

HOAI PHONG NGUYEN, THUAN THANH NGUYEN ✉

Faculty of Electrical Engineering Technology
Industrial University of Ho Chi Minh City
No. 12 Nguyen Van Bao, Ward 4, Go Vap District, Ho Chi Minh City, Vietnam
e-mail: ✉ *nguyenthanhthuan@iuh.edu.vn*

(Received: 06.08.2023, revised: 22.08.2024)

Abstract: Hardware-in-loop (HIL) is a technique that allows one to simulate the behavior of a technical system in real time. This makes it a valuable tool for controller validation in many fields including photovoltaic systems. This paper proposes an experiment solution for maximizing power of the photovoltaic (PV) panel using HIL simulation. The proposed HIL configuration consists of two parts. The first part includes the PV, the DC-DC boost converter and load are simulated using HYPERSIM and run on the real-time OPAL-RT simulator. The second part is the real MPPT controller based on the perturbation and observation (P&O) algorithm for maximum power point tracking (MPPT) using the TMS320F28379D board. To evaluate the effectiveness of the proposed HIL configuration, the paper also presents a software-in-loop (SIL) simulation configuration for MPPT including the PV, the boost converter, load and MPPT controller based on the P&O algorithm which are simulated using HYPERSIM and run on the real-time OPAL-RT simulator. The obtained results by the proposed HIL configuration are compared with those gained by the SIL configuration on the A10J-S72-175 PV module under different irradiance and temperature levels. The obtained results show that the proposed HIL configuration can be used to perform MPPT experiments for PV under different environmental conditions. In addition, the compared results show that the proposed HIL configuration fulfills its usefulness for evaluating the practical MPPT controllers.

Key words: maximum power point tracking, hardware-in-loop, OPAL-RT

Nomenclature

V_{PV}	PV panel voltage
I_{PV}	PV panel current
I_{ph}	Photo generated current
I_0	Reverse saturation current
V_t	Thermal voltage
α	Diode quality factor
ΔV_{PV}	PV voltage fluctuations
ΔI_L	Inductor current ripple
D	PWM duty
ΔD	Step change of PWM duty
SIL	Software-in-loop
HIL	Hardware-in-loop

1. Introduction

1.1. Background

In the context of depleting fossil energy sources and the consequences of environmental pollution, solar energy is becoming increasingly popular worldwide as a renewable energy source due to its cost-effective and environmentally friendly nature [1]. With many environmental benefits such as reducing greenhouse gases like CO_2 and NO_x and technical benefits such as reducing the need for transmission lines and grids, solar energy is considered an ideal energy source for the future [2,3]. However, solar energy, which utilizes photovoltaic (PV) panels to convert sunlight into electricity, requires optimization of the power output as it is a nonlinear power source with output power depending on the load and environmental conditions such as temperature and irradiance. The first challenge to address when using solar energy is the maximum power point tracking (MPPT) control of solar panels. MPPT is a technology of adjusting the load characteristic on the PV to ensure it operates at its maximum power point as external conditions change.

1.2. Literature review

Based on the experiment configurations, there have been numerous studies on optimizing the power output of the PV, which can be categorized into three main approaches consisting of a software-in-loop (SIL), experimentation and hardware-in-loop (HIL). For the first experiment configuration, all of the solar panel, power conversion system and MPPT are built on the simulation software [4]. There are many studies using this method to study the MPPT of PV. In [5,6], the fast MPPT method using the IncMPPT algorithm and back-stepping control is presented through simulations. In [7], the hybrid algorithm golden section search assisted P&O (GSS-PO) is proposed for the MPPT of PV, wherein all of components of the experiment configuration are also built

on MATLAB software. In [8], the modified P&O algorithm with variable step size based on fuzzy control for MPPT is proposed and simulated on MATLAB software. In [9], the artificial neural network (ANN) algorithm for maximum power point tracking applied to a hybrid boost circuit is implemented in MATLAB software. In [10], various advanced algorithms such as fuzzy and ANN combined with PID control are compared for the MPPT of solar panels in a simulation environment. Some works use metaheuristic algorithms for MPPT under different environmental conditions such as particle swarm optimization (PSO) [11], teaching learning based optimization (TLBO) [12], the cat swarm algorithm (CSA) [13] and chimp optimization (ChOA) [14], wherein the entire simulation model and MPPT algorithm are built on the MATLAB/Simulink platform. It can be seen that this research direction can be easily implemented entirely in software. However, due to lack of experimental validation, the reliability when applied in real-world scenarios is still a question.

The second experiment configuration involves experimentation using real solar panels or simulated testbeds and developing hardware for power converters, control units, and control algorithms on microcontrollers. An improved algorithm for P&O is proposed and validated through experimental modeling with the DSP controller TMS320F28379D [15]. In [16], the ANN algorithm is applied for MPPT, wherein the PV module is formulated based on the simulated solar device. In [17], an adaptive PID control model with P&O MPPT is implemented in practical control using an Arduino Uno microcontroller and compared with the proposed simulation results. When using real solar panels, assessing system performance under varying temperature and irradiance becomes challenging due to environmental conditions and measurement devices.

The third experiment configuration combines both simulation and real equipment based on HIL platforms. In [18], the HIL model consisting of the solar energy system under shading conditions and the MPPT based on the cuckoo search algorithm (CS) are proposed using the HIL of the OPAL-RT simulator and DSpace. In [19], the MPPT test system for photovoltaic grid-connected inverter based on the HIL are proposed wherein, the photovoltaic grid-connected inverter model using MATLAB/Simulink is built on the real-time simulator and the MPPT algorithm is implemented on DSpace. In [20], the MPPT algorithm is implemented on the RT-LAB and run on the OPAL-RT simulator while the PV panels and boost circuit are realized by actual hardware. In [21], HIL systems are used in conjunction with control systems based on RT-LAB and MATLAB software to validate the MPPT algorithm for solar panels. The overview of the previous MPPT methods in terms of experimental configurations are summarized in Table 1.

Table 1. Overview of the previous MPPT methods in term of experimental configuration

Method	**SIL**	**HIL**	**Experiment**	**Main results**
Incremental conductance (IncCond) and backstepping control [5, 6]	MATLAB software	none	none	Successful application of IncCond and backstepping control for MPPT
GSS-PO [7]	MATLAB software	none	none	GSS-PO outperforms multi-verse optimization

Continued on next page

Table 1 – *Continued from previous page*

Method	SIL	HIL	Experiment	Main results
Modified P&O with variable step size [8]	MATLAB software	none	none	P&O with variable step outperforms P&O
ANN [9]	MATLAB software	none	none	Successful application of ANN for MPPT
Fuzzy and ANN combined with PID [10]	MATLAB software	none	none	ANN-sliding modes outperforms P&O
PSO [11]	MATLAB software	none	none	PSO outperforms P&O
TLBO [12]	MATLAB software	none	none	TLBO outperforms PSO
CSA [13]	MATLAB software	none	none	CSO outperforms PSO
ChOA [14]	MATLAB software	none	none	ChOA outperforms PSO
Improved P&O [15]	none	none	DSP controller TMS320F28379D	Improved P&O outperforms P&O
ANN [16]			OPAL-RT simulator	
P&O combined with PID [17]	none	none	Arduino	Successful application of P&O combined with PID for MPPT
CS [18]	none	OPAL-RT simulator with RT-LAB and DSpace	none	CSA outperforms PSO
Pulse width modulation [20]	none	OPAL-RT simulator with RT-LAB	none	Successfully performed MPPT experiment on RT-Lab
Improved P&O [21]	none	OPAL-RT simulator with RT-LAB and MC56F8257 controller	none	Improved P&O outperforms P&O and IncCond algorithms.

1.3. Research gap and motivation

The experiment configuration based on HIL offers several prominent advantages such as detecting control algorithm errors, reducing hardware development time for validation, and facilitating system development based on real-time simulation environments [22]. This approach overcomes the disadvantages of two groups of methods SIL and experimentation. Compared to SIL, HIL allows simulation in real time. This makes the controllers fully applicable on real devices after being evaluated on HIL devices. Compared with an experimentation method, HIL allows building large-scale and complex systems without regard to time and cost of building experimental models. Furthermore, the MPPT experiment configuration based on HIL allows performing impact assessments of changing environmental conditions such as temperature and radiation, which are difficult to implement on experimental systems. In addition, model building and editing on HIL is much easier than tuning on real experimentation systems. However, the number of studies using this method has been still very limited. Therefore, it is necessary to encourage studies using HIL to evaluate the effectiveness of MPPT algorithms for PV.

1.4. Contributions

This paper proposes an experimental method for MPPT based on the HIL using an OPAL-RT simulator. The proposed HIL configuration includes the PV, the DC-DC voltage converter circuit and the MPPT controller based on the P&O algorithm, in which, the PV model and boost circuit are built on HYPERSIM software and run on the OPAL-RT HIL system. The MPPT control based on the P&O algorithm is built and run on the TMS320F28379D controller. The MPPT results under different radiation and temperature conditions using the TMS320F28379D controller are compared with the P&O algorithm that is built on HYPERSIM software. The main contributions of this work are as follows:

- Propose the experimental method for MPPT based on the HIL using the OPAL-RT simulator.
- Propose the experimental method for MPPT based on the HIL using the The proposed method for MPPT based on HIL configuration is compared with the method based on the HIL configuration.
- The obtained results under changing environmental conditions show that the proposed HIL configuration can be used to evaluate the effectiveness of real MPPT controllers.

1.5. Paper organization

The paper consists of the following parts: the introduction is presented in this section. The next section shows the proposed HIL configuration. Section 3 shows the obtained results and discussion, and the conclusion of this work is presented in Section 4.

2. The proposed hardware-in-loop simulation configuration

2.1. The PV modeling

The PV panel considered in this study is A10Green Technology A10J-S72-175, which I-V characteristics are dependent on the solar irradiation and ambient temperature as shown in Fig. 1.

The relationship between PV panel voltage (V_{PV}) and current (I_{PV}) can be given as follows [23]:

$$I_{\mathrm{PV}} = I_{ph} - I_0 \cdot \left(e^{\left(\frac{V_{\mathrm{PV}} + R_s \cdot I_{\mathrm{PV}}}{\alpha \cdot V_t} \right)} \right) - \left(\frac{V_{\mathrm{PV}} + R_s \cdot I_{\mathrm{PV}}}{R_{sh}} \right), \tag{1}$$

where: I_{ph} is the photo generated current, V_t is the thermal voltage, I_0 is the reverse saturation current, α is the diode quality factor, R_s is the series resistance, and R_{sh} is the shunt resistance of the PV panel.

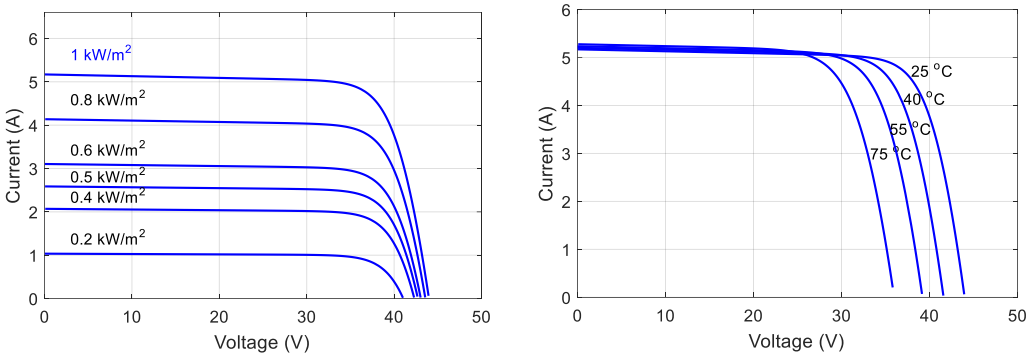

(a) (b)

Fig. 1. The I–V characteristic of A10J-S72-175 Panel: under varying levels of irradiance (a); under varying levels of temperature (b)

The generated photocurrent I_{ph}, the thermal voltage V_t and the reverse saturation current I_0 are determined as follows [10]:

$$I_{ph} = (I_{sc} + K_i \cdot \Delta T) \cdot \frac{G}{1000}, \tag{2}$$

$$V_t = \frac{N_s \cdot K \cdot T}{q}, \tag{3}$$

$$I_0 = \frac{I_{sc} + K \cdot \Delta T}{e^{\left(V_{oc} + \frac{K_V \cdot \Delta T}{\alpha \cdot V_t} \right)}}, \tag{4}$$

where: I_{sc} is the short circuit current at the nominal condition, ΔT is the difference between the actual temperature (T) and nominal temperature (T_n) of the PV, G is the solar irradiation (W/m^2), N_s is the series cells number, K is the Boltzmann constant, q is electrical charge, V_{oc} is the open circuit voltage at the nominal condition, and K_i is the current temperature coefficient.

2.2. The boost converter modeling

The DC-DC converter is used to modify the load characteristics, thereby changing the operating point of the solar panel. In this paper, a boost circuit is applied to adjust the working power of the solar panel by changing the modulation ratio of the switching on-off presented in Fig. 2.

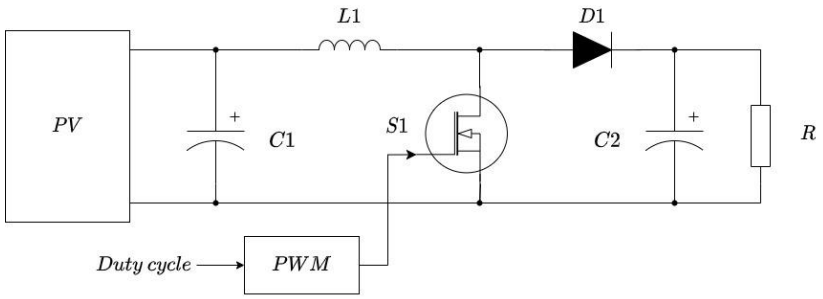

Fig. 2. Boost DC-DC converter

It is evident that when the load is fixed, the operating point can vary with the intensity of irradiance, as shown in Fig. 3. Furthermore, if at a certain irradiance level, the power reaches its maximum, then when the irradiance changes, the power will no longer reach its maximum. Therefore, it is necessary to modify the load characteristics using a boost circuit with adjustable output voltage or control according to the modulation ratio and apply a maximum power point tracking algorithm. The relationship between the output voltage (V_{DC}) and the solar panel voltage is presented in the below equation.

$$V_{\mathrm{DC}} = \frac{V_{\mathrm{PV}}}{1 - D}, \tag{5}$$

where D is the duty cycle.

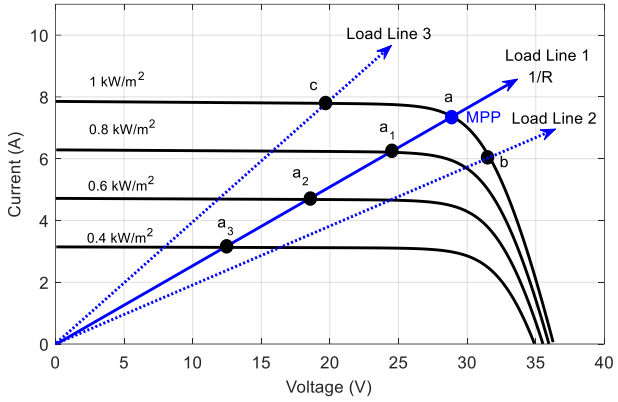

Fig. 3. The operating point of the PV under different load conditions

The parameters of the boost circuit affect the voltage and current fluctuations across the elements. The value of the inductor (L) is chosen based on the voltage fluctuations (ΔV_{PV}) of the solar panel and the current ripple (ΔI_L) on the inductor as follows [10]:

$$L = \frac{\Delta V_{\mathrm{PV}}}{f \cdot \Delta I_L}, \tag{6}$$

where f is the cutoff frequency of the semiconductor switch.

Capacitors C_1 and C_2 are selected based on the voltage ripple ΔV_{PV}, ΔV_{DC} and the current ripple (ΔI_{DC}) as follows:

$$\begin{cases} C_1 = \dfrac{\Delta V_{\mathrm{PV}}}{8 \cdot L \cdot \Delta V_{\mathrm{PV}} \cdot f^2} \\ C_2 = \dfrac{\Delta I_{\mathrm{DC}}}{f \cdot \Delta V_{\mathrm{DC}}} \end{cases}. \tag{7}$$

2.3. The P&O MPPT algorithm

Under the influence of temperature, irradiance and load variations, the non-linear characteristic of the PV panel forces the output power to operate at a specific power point. To keep the PV operation power at the maximum power point, a DC-DC power converter is used to modify the load characteristics and adjust the working point of the PV. In addition, a search algorithm is employed to calculate the pulse width modulation (PWM) value for the power converter.

Among many MPPT methods, the P&O algorithm is widely applied due to its simplicity and effectiveness [8, 24]. This technique continuously varies the pulse width of the power converter to create perturbations in the output power, from which the optimal pulse width value is calculated and the output power is controlled to oscillate around the maximum power point.

The P&O algorithm is depicted in the flowchart as shown in Fig. 4, wherein ΔD represents the step change made in each iteration to perform the maximum power point tracking.

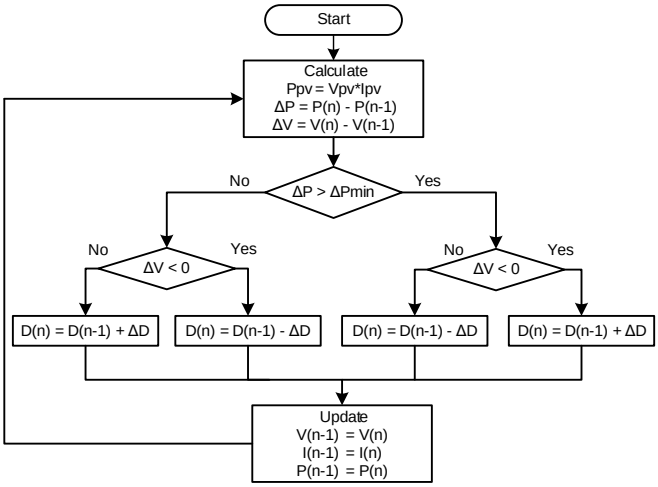

Fig. 4. Flowchart of the P&O algorithm

2.4. The proposed HIL configuration

HIL simulation for the solar panel MPPT problem brings numerous benefits such as reducing equipment investment costs, avoiding undesired weather influences to analyze experimental results and expanding of experimental systems [19, 25, 26]. An HIL system consists of an HIL simulator and an embedded system implementing the algorithm [27] which are connected together through input and output interfaces as shown in Fig. 5.

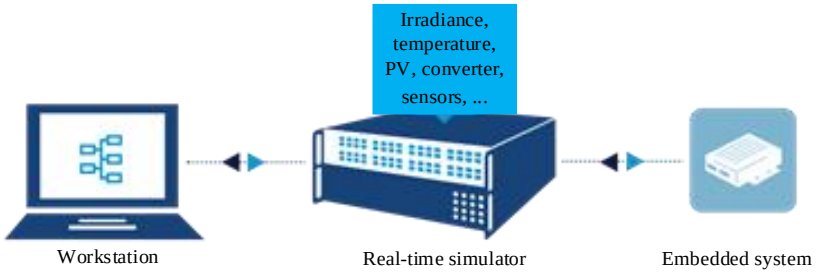

Fig. 5. Structure of the HIL system

In this work, the proposed HIL configuration involves two parts. The first part consists of the HIL simulation of the solar panel and power circuit. The simulation model is built on HYPERSIM software version 2021.3 and run on the OPAL-RT 5707XG with Intel Xeon 16 cores, 3.3 GHz, 32 GB RAM, 512 GB SSD and HIL Virtex®-7 FPGA-based Real-Time Simulator. The analogue input card OP5340 and output card OP5330 are integrated with the system to export and import signals from/to the HIL system. The proposed simulation MPPT model is shown in Fig. 6.

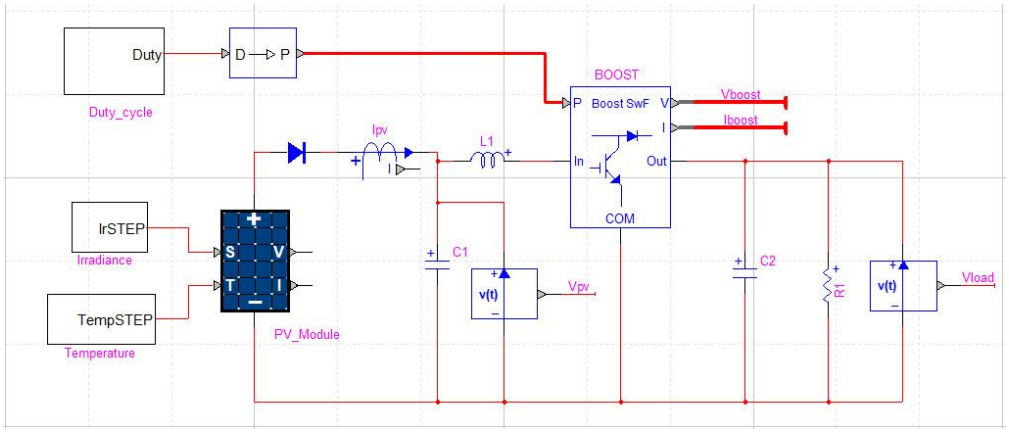

Fig. 6. MPPT simulation model for solar panel on HYPERSIM software

The second part is the DSP controller C2000 TMS320F28379D from Texas Instrument, which is used to read the current and voltage signals of the solar panel and execute the MPPT algorithm to find the optimal pulse width to control the switching of the power circuit in the HIL setup. The entire proposed HIL configuration for the MPPT of PV is shown in Fig. 7.

The connection of signals between the TMS320F28379D controller and the OP5707XG simulator as well as the hardware configuration in HYPERSIM software is shown in Fig. 8, where the current and voltage of the PV on the simulation model are respectively exported to channel 0 and channel 1 of the OP5340 in Slot 1A of the OP5707XG simulator. The duty cycle signal is read from channel 1 of the OP5330 in Slot 1B of the OP5707XG simulator. The experimental system for the MPPT of PV based on HIL is shown in Fig. 9.

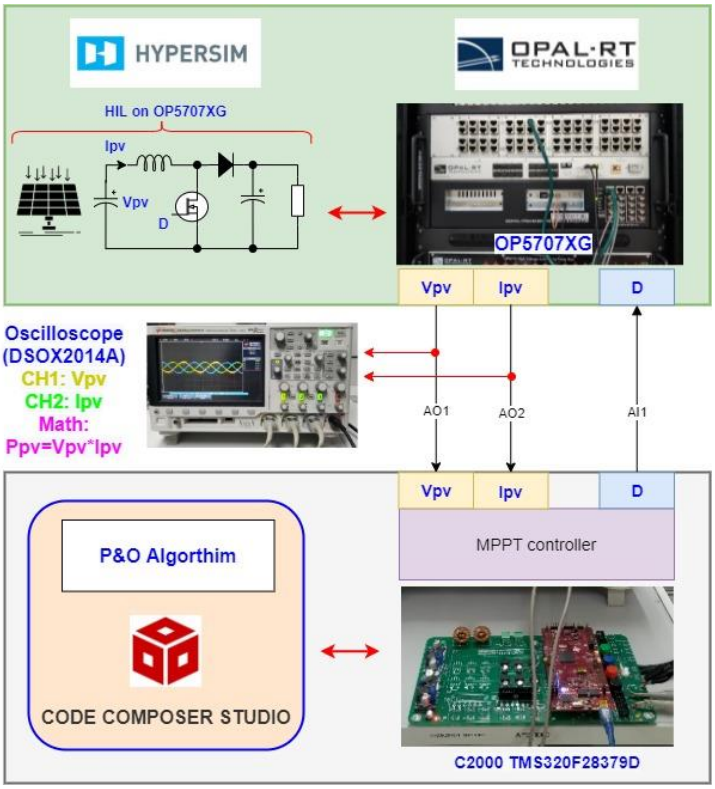

Fig. 7. The proposed HIL configuration for MPPT of PV

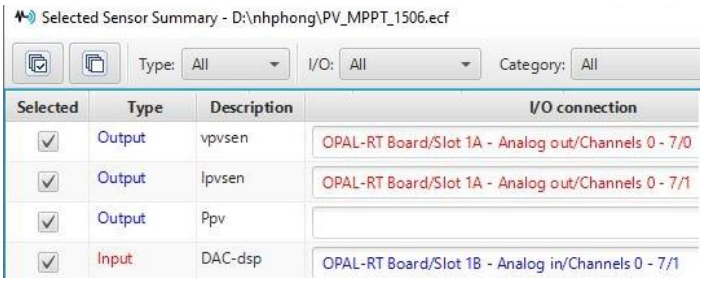

(a)

(b)

Fig. 8. Hardware configuration for OP5707XG: signal pin configuration in the HYPERSIM software (a); connecting the OP5707XG hardware and TMS320F28379D (b)

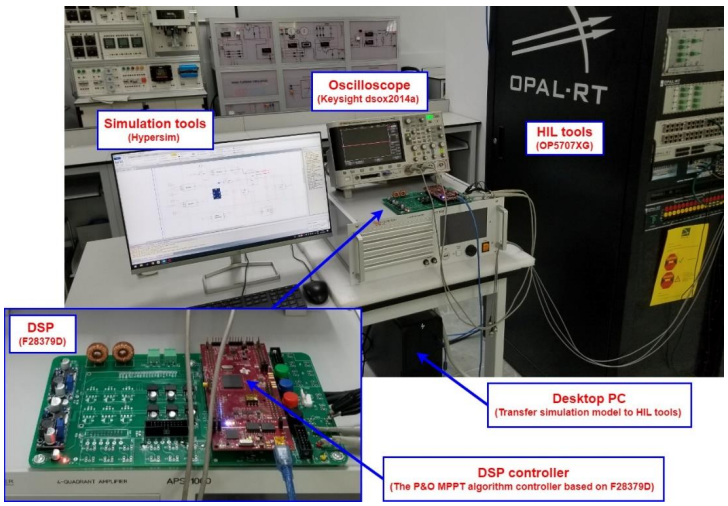

Fig. 9. The HIL experimental setup on OPAL-RT 5707XG and DSP TMS320F28379D

3. Result and discussion

To evaluate the effectiveness of the proposed HIL configuration for the MPPT of PV, the MPPT results obtained from the proposed configuration are compared with the MPPT results obtained from the SIL where all of parts consisting of the PV model, power circuit and P&O MPPT algorithm are built on HYPERSIM software and run entirely on OPAL-RT 5707XG simulator. The P&O algorithm for the MPPT implemented on HYPERSIM software is shown in Fig. 10. It can be seen that for both methods, the power part uses software-based simulation. The control algorithm part of the system is divided into two parts. For the proposed HIL configuration, the control algorithm is embedded on the external hardware using TMS320F28379D. For the SIL configuration, the control algorithm is simulated using the HYPERSIM software.

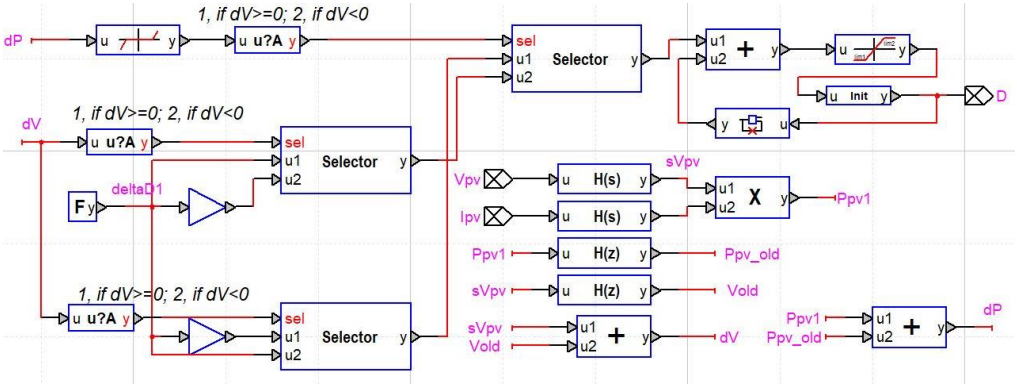

Fig. 10. The P&O algorithm implemented on HYPERSIM software for SIL configuration

The parameters of the boost circuit are calculated using Formulas (2) and (3) with a switching frequency of 5 kHz, and the voltage ripple of the solar panel $\Delta V_{\mathrm{PV}} < 5\%$ and the inductor current ripple $\Delta I_L < 20\%$. The results are as follows: $C_1 = 220$ µF, $C_2 = 470$ µF, $L = 2$ mH, $R = 50$ Ω. The parameters of the P&O algorithm used for both HIL and SIL configurations are presented in Table 2.

Table 2. Parameter of P&O MPPT simulation

Parameter	Abbreviation	Value
Duty cycle max	$D_{\max}$	0.8
Duty cycle min	$D_{\min}$	0.1
Initial duty cycle	D_{init}	0.5
Perturbation value	ΔD	3e-3
MPPT loop rate	f_{MPPT}	100 Hz

The experiment evaluates the system response with the A10J-S72-175 solar panel under different conditions of varying irradiance and temperature. The A10J-S72-175 module has the parameters consisting of a maximum power of 175.0914 W, an open circuit voltage of 43.99 V, a short-circuit current of 5.17 A, voltage and current at a maximum power point of 36.63 V and 4.78 A, respectively. Its power-voltage characteristics under different irradiance and temperature are depicted in Fig. 11. The following test cases are considered:

Test case 1: The irradiance varies at each level [0.2; 0.4; 0.6; 0.8; 1; 0.5] kW/m^2.

Test case 2: The temperature varies at each level [70; 55; 40; 25]°.

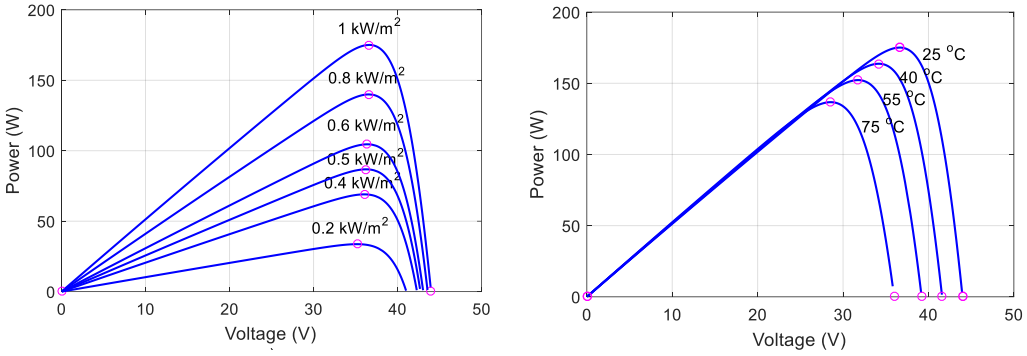

Fig. 11. The P–V characteristic of A10J-S72-175 Panel: under varying levels of irradiance (a); under varying levels of temperature (b)

For case 1, Fig. 12 illustrates the power and voltage of PV, and the duty cycle of the system when the irradiance changes according to {0.2, 0.4, 0.6, 0.8, 1, and 0.5 kW/m^2} at temperature 25°. The waveform in blue represents the SIL simulation data, while the waveform in red represents the data from the HIL experiment. From the figure, the results gained by SIL on an OPAL-RT

5707XG simulator and HIL are similar. From the figure, the maximum power obtained on PV at temperature 25° with radiation levels of $\{1, 0.8, 0.6, 0.5, 0.4, 0.4$ and 0.2 kW/m$^2\}$ are about 175, 140, 105, 87, 69 and 34 W, respectively. These results are completely similar to the decompressed data from Fig. 11(a). Both of configurations find the maximum working point of PV after about 0.1–0.3 s after changing the irradiance level. The optimal power and voltage of PV gained by two configurations as well as the optimal pulse width established for each radiation level of both methods are the same. The results on HIL show minor fluctuations compared to SIL due to noise on the analogue input readings to a TMS320F28379D microcontroller and the duty signal from a TMS320F28379D microcontroller to the OP5707XG simulator. These results show that the proposed HIL configuration is completely feasible to evaluate the efficiency of MPPT algorithms on the real controllers. The results also show that the proposed HIL configuration has ablity to validate the operation of the real MPPT controller under different irradiance levels.

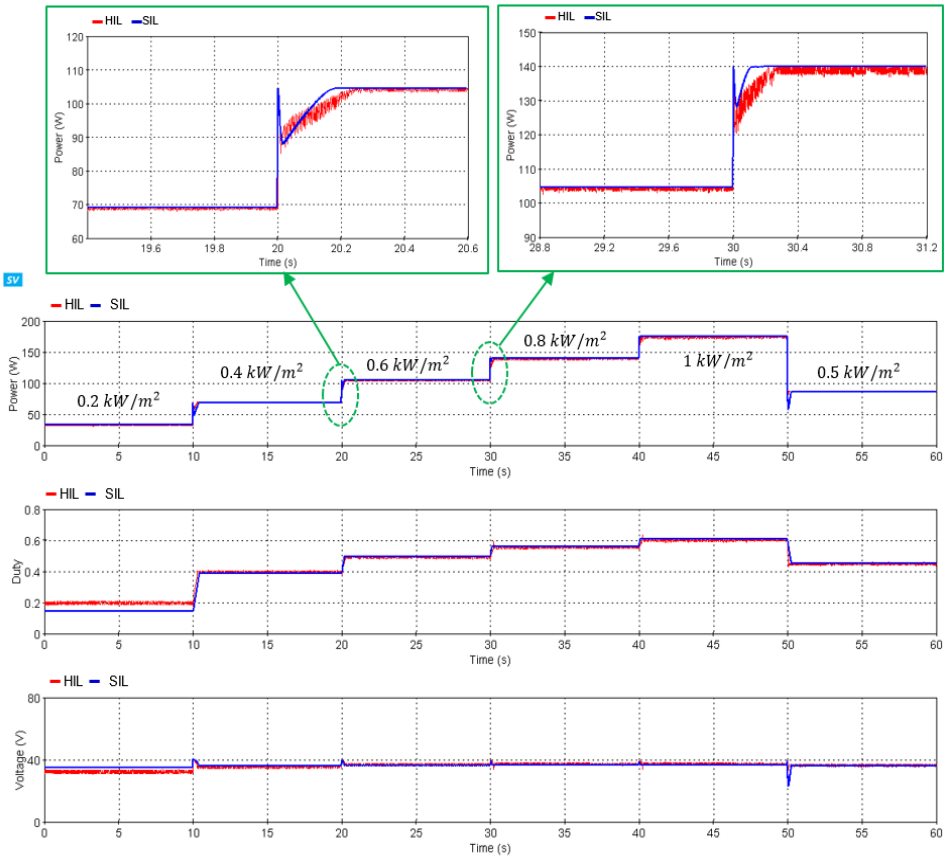

Fig. 12. The response of P_{pv}, V_{pv}, and D of the HIL and SIL configurations under different irradiance levels

Figure 13 shows the real waveform observed on the oscilloscope. The yellow line represents the voltage of the solar panel, the green line represents the current of the PV, and the pink line represents the power of the PV. These signal values are the same as the signal values that are

displayed on the scope view of HYPERSIM as shown in Fig. 12. The results obtained on the oscilloscope show that using the proposed HIL configuration allows the acquisition of the actual signal values on the PV.

Fig. 13. The response of PV power, voltage and current for different irradiance levels obtained by the HIL configuration on the oscilloscope

For case 2, Fig. 14 illustrates the power and voltage of PV, and duty cycle of the system when the when temperature changes according to $\{70, 55, 40, \text{and } 25°\}$ at an irradiance of 1.0 kW/m^2.

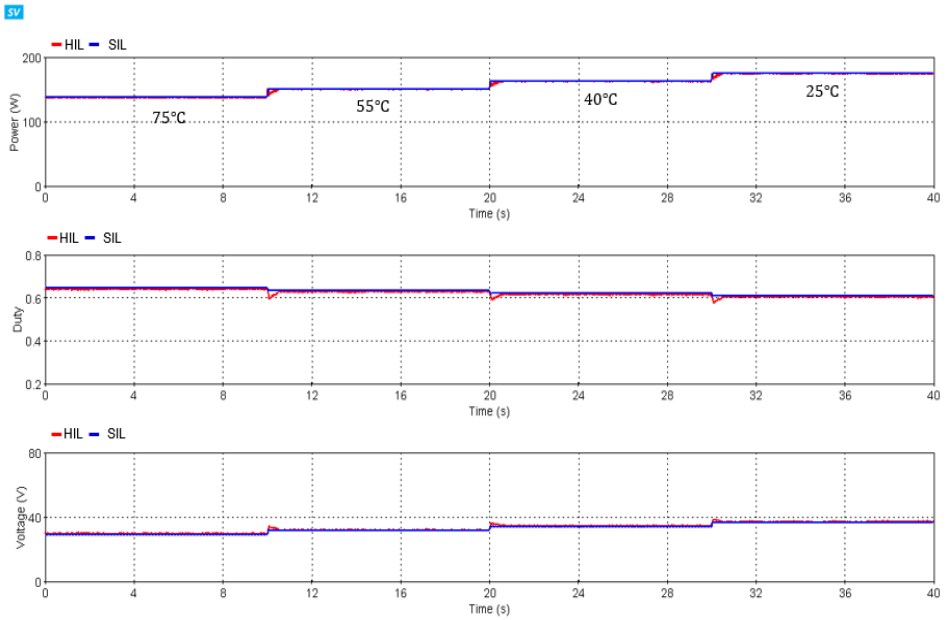

Fig. 14. The response of P_{pv}, V_{pv}, and D of the HIL and SIL configurations under different temperature levels

The figure shows that the results gained by SIL on a OPAL-RT 5707XG simulator and HIL are similar. The maximum power obtained on PV at the radiation level of 1.0 kW/m^2 and the temperature levels of {75, 55, 40 and 25°} are 137 152, 164 and 175 W, respectively. This result is completely similar to decompressed data from Fig. 11(b). This once again shows that the proposed HIL configuration helps to validate the operation of the real MPPT controller under different temperature conditions of the PV. Furthermore, the real waveform of power, voltage and current of the PV for this case is also shown in Fig. 15.

Fig. 15. The response of PV power, voltage and current for different temperature levels obtained by the HIL configuration on the oscilloscope

4. Conclusion

The article proposes a practical solution for maximizing power of the PV using HIL simulation to enhance the practicality of MPPT research for PV. The proposed HIL configuration consists of two parts. The first part includes the PV, the boost converter and load are simulated using HYPERSIM and run on the real-time OPAL-RT simulator, while the second part is the real MPPT controller using the TMS320F28379D board. The obtained results by the proposed HIL configuration are compared with the SIL configuration, which contains all two parts and runs on the real-time OPAL-RT simulator. The comparison results between HIL and SIL simulation under different irradiance and temperature levels are similar. The power obtained on PV with the radiation levels of {1, 0.8, 0.6, 0.5, 0.4, 0.4 and 0.2 kW/m^2} at temperature 25° and {75, 55, 40 and 25°} at a radiation level of 1.0 kW/m^2 are {175, 140, 105, 87, 69 and 34 W} and {137152, 164 and 175 W} respectively, which is similar to the decompressed data from the PV datasheet. The results also show that using the proposed HIL configuration makes it easy to evaluate the effectiveness of real MPPT controllers under changing environmental conditions, which is not easily implemented for real PV systems. Furthermore, the physical signals of voltage, current and power of PV obtained from the HIL configuration are completely the same as those from the simulation results. Therefore, the proposed HIL configuration is suitable for experimental verification of various algorithms inside the real controllers. For future works, the proposed HIL configuration can be combined with power devices to form the power HIL configuration which allows one to test both the real controller and the boost converter.

References

[1] Nagadurga T., Narasimham P.V.R.L., Vakula V.S., Devarapalli R., *Gray wolf optimization-based optimal grid connected solar photovoltaic system with enhanced power quality features*, Concurrency and Computation: Practice and Experience, vol. 34, no. 5, e6696 (2022), DOI: 10.1002/cpe.6696.

[2] Sutikno T., Cahya Subrata A., Pau G., Jusoh A., Ishaque K., *Maximum power point tracking techniques for low-cost solar photovoltaic applications–Part I: constant parameters and trial-and-error*, Archives of Electrical Engineering, vol. 72, no. 1, pp. 125–145 (2023), DOI: 10.24425/aee.2023.143693.

[3] Dahlan U.A., Bahru J., *Maximum power point tracking techniques for low-cost solar photovoltaic applications – Part II: Mathematical Calculation and Measurement and Comparison, criteria on choices and suitable MPPT techniques*, Archives of Electrical Engineering, vol. 72, no. 2, pp. 299–322 (2023), DOI: 10.24425/aee.2023.145410.

[4] Gómez-Luna E., Palacios-Bocanegra L., Candelo-Becerra J.E., *Real-time Simulation with OPAL-RT Technologies and Applications for Control and Protection Schemes in Electrical Networks*, Journal of Engineering Science & Technology Review, vol. 12, no. 3 (2019).

[5] Moutchou M., Jbari A., *Fast photovoltaic IncCond-MPPT and backstepping control, using DC-DC boost converter*, International Journal of Electrical and Computer Engineering (IJECE), vol. 10, no. 1, pp. 1101–1112 (2020), DOI: 10.11591/ijece.v10i1.pp1101-1112.

[6] Diouri O., Es-Sbai N., Errahimi F., Gaga A., Alaoui C., *Modeling and design of single-phase PV inverter with MPPT algorithm applied to the boost converter using back-stepping control in standalone mode*, International Journal of Photoenergy, vol. 2019 (2019), DOI: 10.1155/2019/7021578.

[7] Mostafa H.H., Ibrahim A.M., Anis W.R., *A performance analysis of a hybrid golden section search methodology and a nature-inspired algorithm for MPPT in a solar PV system*, Archives of Electrical Engineering, vol. 68, no. 3, pp. 611–627 (2019), DOI: 10.24425/aee.2019.129345.

[8] Sibtain D., Gulzar M.M., Shahid K., Javed I., Murawwat S., Hussain M.M., *Stability analysis and design of variable step-size P&O algorithm based on fuzzy robust tracking of MPPT for standalone/grid connected power system*, Sustainability, vol. 14, no. 15, 8986 (2022), DOI: 10.3390/su14158986.

[9] Haseeb I., Armghan A., Khan W., Alenezi F., Alnaim N., Ali F., Muhammad F., Albogamy F.R., Ullah N., *Solar power system assessments using ann and hybrid boost converter based MPPT algorithm*, Applied Sciences, vol. 11, no. 23, 11332 (2021), DOI: 10.3390/app112311332.

[10] Zdiri M.A., Khelifi B., Salem F. Ben, Abdallah H.H., *A Comparative Study of Distinct Advanced MPPT Algorithms for a PV Boost Converter*, International Journal of Renewable Energy Research (IJRER), vol. 11, no. 3, pp. 1156–1165 (2021), DOI: 10.20508/ijrer.v11i3.12079.g8282.

[11] Nagadurga T., Narasimham P.V.R.L., Vakula V.S., *Harness of maximum solar energy from solar PV strings using particle swarm optimisation technique*, International Journal of Ambient Energy, vol. 42, no. 13, pp. 1506–1515 (2021), DOI: 10.1080/01430750.2019.1611643.

[12] Nagadurga T., Narasimham P.V.R.L., Vakula V.S., *Global maximum power point tracking of solar PV strings using the teaching learning based optimisation technique*, International Journal of Ambient Energy, vol. 43, no. 1, pp. 1883–1894 (2022), DOI: 10.1080/01430750.2020.1721327.

[13] Nagadurga T., Narasimham P.V.R.L., Vakula V.S., *Global maximum power point tracking of solar photovoltaic strings under partial shading conditions using cat swarm optimization technique*, Sustainability (Switzerland), vol. 13, no. 19 (2021), DOI: 10.3390/su131911106.

[14] Nagadurga T., Lakshmi Narasimham P.V.R., Vakula V.S., Devarapalli R., García Márquez F.P., *Enhancing global maximum power point of solar photovoltaic strings under partial shading conditions using chimp optimization algorithm*, Energies, vol. 14, no. 14 (2021), DOI: 10.3390/en14144086.

[15] Raiker G.A., Loganathan U., *Current control of boost converter for PV interface with momentum-based perturb and observe MPPT*, IEEE Transactions on Industry Applications, vol. 57, no. 4, pp. 4071–4079 (2021), DOI: 10.1109/tia.2021.3081519.

[16] Khan M.J., Mathew L., *Artificial neural network-based maximum power point tracking controller for real-time hybrid renewable energy system*, Soft Computing, vol. 25, pp. 6557–6575 (2021), DOI: 10.1007/s00500-021-05653-0.

[17] Sahoo J., Samanta S., Bhattacharyya S., *Adaptive PID controller with P&O MPPT algorithm for photovoltaic system*, IETE Journal of Research, vol. 66, no. 4, pp. 442–453 (2020), DOI: 10.1080/03772063.2018.1497552.

[18] Al-Shammaa A.A.M., Abdurraqeeb A., Noman A.M., Alkuhayli A., Farh H.M.H., *Hardware-In-the-Loop Validation of Direct MPPT Based Cuckoo Search Optimization for Partially Shaded Photovoltaic System*, Electronics, vol. 11, no. 10, p. 1655 (2022), DOI: 10.3390/electronics11101655.

[19] Huang W., Shu M., Li T., Sun Y., Ma L., *MPPT test based on hardware-in-the-loop simulation platform of photovoltaic systems*, in 2020 IEEE 3rd International Conference on Electronics Technology (ICET), pp. 463–466 (2020), DOI: 10.1109/icet49382.2020.9119670.

[20] Xiaodong Y., Yan Z., Weiping Z., *Real-time simulation and research on photovoltaic power system based on RT-LAB*, The Open Fuels & Energy Science Journal, vol. 8, no. 1, pp. 183–188 (2015).

[21] Zhang K., *Control simulation and experimental verification of maximum power point tracking based on rt-lab*, International Journal of Engineering, vol. 29, no. 10, pp. 1372–1379 (2016.

[22] Noureen S.S., Roy V., Bayne S.B., *An overall study of a real-time simulator and application of RT-LAB using MATLAB simpowersystems*, in 2017 IEEE green energy and smart systems conference (IGESSC), IEEE, pp. 1–5 (2017), DOI: 10.1109/igesc.2017.8283453.

[23] Zhang Z., Song G., Zhou J., Zhang X., Yang B., Liu C., Guerrero J.M., *An adaptive backstepping control to ensure the stability and robustness for boost power converter in DC microgrids*, Energy Reports, vol. 8, pp. 1110–1124 (2022), DOI: 10.1016/j.egyr.2022.02.024.

[24] Basha C.H.H., Rani C., *Different conventional and soft computing MPPT techniques for solar PV systems with high step-up boost converters: A comprehensive analysis*, Energies, vol. 13, no. 2, 371 (2020), DOI: 10.3390/en13020371.

[25] Samano-Ortega V., Padilla-Medina A., Bravo-Sanchez M., Rodriguez-Segura E., Jimenez-Garibay A., Martinez-Nolasco J., *Hardware in the loop platform for testing photovoltaic system control*, Applied Sciences, vol. 10, no. 23, 8690 (2020), DOI: 10.3390/app10238690.

[26] Khazaei J., Miao Z., Piyasinghe L., Fan L., *Real-time digital simulation-based modeling of a single-phase single-stage PV system*, Electric Power Systems Research, vol. 123, pp. 85–91 (2015), DOI: 10.1016/j.epsr.2015.01.023.

[27] Mihalič F., Truntič M., Hren A., *Hardware-in-the-loop simulations: A historical overview of engineering challenges*, Electronics, vol. 11, no. 15, 2462 (2022), DOI: 10.3390/electronics11152462.